Atmospheric
Chemistry
and Physics
Discussions

1 # Primary emissions versus secondary formation of fine particulate matter in the top polluted

2 city, Shijiazhuang, in North China

3 Ru-Jin Huang[1], Yichen Wang[1], Junji Cao[1], Chunshui Lin[1,2], Jing Duan[1], Qi Chen[3], Yongjie Li[4],

4 Yifang Gu[1], Jin Yan[1], Wei Xu[1,2], Roman Fröhlich[5], Francesco Canonaco[5], Carlo Bozzetti[5], Jurgita

5 Ovadnevaite[2], Darius Ceburnis[2], Manjula R. Canagaratna[6], John Jayne[6], Douglas R. Worsnop[6], Imad

6 El-Haddad[5], André S. H. Prévôt[5], Colin D. O'Dowd[2]

7 [1]Key Laboratory of Aerosol Chemistry & Physics, State Key Laboratory of Loess and Quaternary

8 Geology, Institute of Earth Environment, Chinese Academy of Sciences, Xi'an 710061, China

9 [2]School of Physics and Centre for Climate and Air Pollution Studies, National University of Ireland

10 Galway, Galway, Ireland

11 [3]State Key Joint Laboratory of Environmental Simulation and Pollution Control, College of

12 Environmental Sciences and Engineering, Peking University, Beijing, China

13 [4]Department of Civil and Environmental Engineering, Faculty of Science and Technology, University

14 of Macau, Taipa, Macau, China

15 [5]Laboratory of Atmospheric Chemistry, Paul Scherrer Institute (PSI), 5232 Villigen, Switzerland

16 [6]Aerodyne Research, Inc., Billerica, MA, USA

17 *Correspondence to*: R.-J. Huang (rujin.huang@ieecas.cn)

18 **Abstract.** Particulate matter (PM) pollution is a severe environmental problem in the Beijing-Tianjin-

19 Hebei (BTH) region in North China. PM studies have been conducted extensively in Beijing, but the

20 chemical composition, sources, and atmospheric processes of PM are still relatively less known in the

21 nearby Tianjin and Hebei. In this study, fine PM in urban Shijiazhuang (the capital of Hebei province)

22 was characterized using an Aerodyne quadrupole aerosol chemical speciation monitor (Q-ACSM)

23 from 11 January to 18 February in 2014. The average mass concentration of non-refractory submicron

24 PM (diameter <1 μm, NR-PM$_1$) was 178 ± 101 μg m^{-3} and composed of 50% organic aerosol (OA),

25 21% sulfate, 12% nitrate, 11% ammonium, and 6% chloride. Using the Multilinear Engine (ME-2)

Atmospheric
Chemistry
and Physics
Discussions

1   receptor model, five OA sources were identified and quantified, including hydrocarbon-like OA from

2   vehicle emissions (HOA, 13%), cooking OA (COA, 16%), biomass burning OA (BBOA, 17%), coal

3   combustion OA (CCOA, 27%), and oxygenated OA (OOA, 27%). We found that secondary

4   formation contributed substantially to PM in episodic events, while primary emissions were dominant

5   (most significant) on average. The episodic events with the highest $NR\text{-}PM_1$ mass range of 300-360

6    $\mu g \ m^{-3}$ showed 55% of secondary species. On the contrary, a campaign-average low OOA fraction

7   (27%) in OA indicated the importance of primary emissions, and a low sulfur oxidation degree (F_{SO4})

8   of 0.18 even at RH>90% hinted on insufficient oxidation. These results suggested that in wintertime

9   Shijiazhuang fine PM was mostly from primary emissions without sufficient atmospheric aging,

10   indicating opportunities for air quality improvement by mitigating direct emissions. In addition,

11   secondary inorganic and organic (OOA) species dominated in pollution events with high RH

12   conditions, most likely due to enhanced aqueous-phase chemistry, while primary organic aerosol

13   (POA) dominated in pollution events with low RH and stagnant conditions. These results also

14   highlighted the importance of meteorological conditions for PM pollution in this highly polluted city

15   in North China.

16   **1 Introduction**

17   Particulate pollution in China is a serious environmental problem, influencing air quality, regional and

18   global climate and human health. Especially during recent winters, large-scale and severe haze

19   pollution has brought China's particulate pollution at the forefront of world-wide media and evoking

20   great scientific interest in air pollution studies. Measurements at a number of major cities showed that

21   the wintertime daily average mass concentration of $PM_{2.5}$ (particulate matter with an aerodynamic

22   diameter <2.5 µm) are approximately 1-2 orders of magnitude higher than those observed in urban

23   areas in the US and European countries (Huang et al., 2014). Severe particulate pollution is often

24   accompanied by extremely poor visibility and poor air quality leading to a sharp increase in

25   respiratory diseases. Long-term exposure to high levels of particulate pollution is estimated to result

26   in 1.36 million premature deaths per year in China, ranking the 1st in the world (Lelieveld et al.,

27   2015).

Atmospheric
Chemistry
and Physics
Discussions

1   The region of Beijing, Tianjin, and Hebei (BTH) is one of the important city clusters in China, but

2   also suffers from serious air pollution. Seven cities in this region ranked the top 10 most polluted

3   cities in China in the year 2014-2015 (http://www.zhb.gov.cn). The urgent need of an air quality

4   improvement in this region has been recognized by central and local governments as well as the

5   public, leading to mitigating actions being undertaken by the authorities. In particular, various

6   emission control measures were implemented in this region to clean Beijing's sky, for example,

7   during the 2014 Asia-Pacific Economic Cooperation (APEC) summit. These temporal measures

8   include the odd-even ban on vehicles and shutdowns of factories and construction sites, leading to

9   serious side effects on daily life and economic growth. Therefore, identification of the major sources

10   and atmospheric processes producing airborne particles is required for implementing targeted and

11   optimized emission control strategies.

12   The first step for quantifying the PM sources requires the measurements of inorganic and organic

13   tracers and/or mass spectrometric fingerprints of ambient PM samples. This can be realized by the

14   online ambient measurements using aerosol mass spectrometric (AMS) techniques to determine

15   aerosol composition (Jimenez et al., 2009; Ng et al., 2011b; Elser et al., 2016b). In particular, the

16   quadrupole aerosol chemical speciation monitor (Q-ACSM) and recently time-of-flight aerosol

17   chemical speciation monitor (TOF-ACSM) have been developed for long-term continuous

18   measurements of the non-refractory submicron aerosols (Ng et al., 2011a; Fröhlich et al., 2013).

19   Aerosol sources have been successfully identified from the AMS measurements with positive matrix

20   factorization (PMF) analysis (Ulbrich et al., 2009; Crippa et al., 2013; Elser et al., 2016a). In terms of

21   Q-ACSM datasets, the use of PMF often fails to resolve sources with similar mass spectral profiles,

22   e.g. the mixing of cooking organic aerosol with traffic organic aerosol in Nanjing (Zhang et al.,

23   2015b); or those present in low contributions, e.g. the lack of success in resolving a factor related to

24   biomass burning in Beijing (Jiang et al., 2015). It was also pointed out that PMF cannot separate the

25   aerosol sources of temporal covariations driven by low temperature and periods of strong inversions

26   (Canonaco et al., 2013; Reyes et al., 2016). Several source apportionment studies (in which PMF did

27   not find optimal results) have utilized the multilinear engine (ME-2) solver, which enables constraint

28   of the factor profiles/time series, providing a superior separation of the PM sources in Europe (e.g.,

Atmospheric
Chemistry
and Physics
Discussions

1   Canonaco et al., 2013; Canonaco et al., 2015; Fröhlich et al., 2015a; Fröhlich et al., 2015b;

2   Minguillón et al., 2015; Petit et al., 2015; Ripoll et al., 2015; Reyes et al., 2016; Bressi et al., 2016;

3   Schlag et al., 2016). However, studies using ME-2 to resolve OA sources from the ACSM

4   measurements are scarce in the BTH region.

5   Apart from the lack of applications of ME-2 for the OA source apportionment, most of the field

6   studies have mainly focused on the aerosol pollution in Beijing (Sun et al., 2013; Sun et al., 2014; Sun

7   et al., 2016; Jiang et al., 2015; Xu et al., 2015; Elser et al., 2016b; Hu et al., 2016a). These and related

8   studies have clearly shown that Beijing is sensitive to the regional transport of aerosols from its

9   surrounding areas (Xu et al., 2008; Zhang et al., 2012; Li et al., 2015a). For example, Guo et al.

10   (2010) estimated that the regional pollutants on average accounted for 69% of PM_{10} and 87% of $PM_{1.8}$

11   in Beijing during summer, with sulfate, ammonium, and oxalate mostly formed regionally (regional

12   contributions >87%). Sun et al. (2014) reported that 66% of $NR\text{-}PM_1$ was from regional transport in

13   Beijing during the 2013 winter haze event. Among the surrounding areas of Beijing, the Hebei

14   province is the main source area leading to high aerosol loadings in Beijing (Chen et al., 2007; Xu et

15   al., 2008; Lang et al., 2013; Li et al., 2015a).

16   Shijiazhuang, the capital of Hebei province, is located ~270 km south of Beijing and has a population

17   approximately half that of Beijing. Zhao et al. (2013a, b) characterized the spatial and seasonal

18   variations of $PM_{2.5}$ chemical composition in the BTH region, and Shijiazhuang was selected as the

19   representative of the polluted cities in Hebei province. The off-line analysis results showed that

20   organic carbon (OC) and elemental carbon (EC) concentrations in Shijiazhuang were lower in the

21   spring and summer than those in the autumn and winter. The sum of secondary inorganic species

22   (SO_4^{2-}, NO_3^-, and NH_4^+) was highest in the autumn. Yet the temporal profiles of PM composition

23   cannot be captured by off-line analyses, hindering more detailed study on the sources and formation

24   of PM. In this work, we present for the first time the 30-minute time resolved $NR\text{-}PM_1$ measurements

25   in Shijiazhuang during the winter heating season. The characteristics of $NR\text{-}PM_1$ are analyzed, which

26   include (1) time series, mass fraction and diurnal variation of $NR\text{-}PM_1$ species; (2) multilinear engine

27   (ME-2)-resolved OA sources and their mass fraction as well as their diurnal variation; and (3) the

Atmospheric
Chemistry
and Physics
Discussions

1   characteristics and atmospheric evolution of aerosol composition and sources under different aerosol

2   loadings and meteorological conditions.

3   **2 Methods**

4   **2.1 Sampling site**

5   Shijiazhuang, the capital of Hebei province, is located ~270 km south of Beijing. In 2014, ~10 million

6   residents and 2.1 million vehicles were reported in this city. It is often ranked the first in the list of top

7   10 most polluted cities in China, especially during wintertime heating periods (from 15 November to

8   15 March next year). For example, the average concentration of $PM_{2.5}$ was 226.5 µg m^{-3} with the

9   peak hourly concentration of 933 µg m^{-3} during the 2013/3014 wintertime heating period, largely

10 exceeding the Chinese air pollution limit of 75 µg m^{-3}. In this study, we performed an intensive field

11 measurement campaign at an urban site in Shijiazhuang to investigate the chemical composition,

12 sources and atmospheric processes of fine particles. The campaign was carried out from 11 January to

13 18 February 2014 on the building roof (15 m) of the Institute of Genetics and Developmental Biology,

14 Chinese Academy of Sciences (38°2'3''N, 114°32'29''E), a site located in a residential-business

15 mixed zone.

16 **2.2 Instrumentation**

17 $NR-PM_1$ was measured with an Aerodyne quadrupole aerosol chemical speciation monitor (Q-

18 ACSM), which can provide quantitative mass concentration and mass spectra of non-refractory

19 species including organics, sulfate, nitrate, ammonium, and chloride. The operation principles of Q-

20 ACSM can be found elsewhere (Ng et al., 2011a). The ambient aerosol was drawn through a Nafion

21 dryer (Perma Pure PD-50T-24SS) following a URG cyclone (Model: URG-2000-30ED) with a cut-off

22 size of 2.5 µm to remove coarse particles. The sampling flow was ~3 L min^{-1}, of which ~85 mL min^{-1}

23 was isokinetically sampled into the Q-ACSM. The residence time in the sampling tube was ~5 s. The

24 Q-ACSM was operated with a time resolution of 30 min and scanned from m/z 10 to 150 at 200 ms

25 amu^{-1}. Dry mono-dispersed 300-nm ammonium nitrate and ammonium sulfate particles (selected by a

26 differential mobility analyzer, DMA, TSI model 3080) were nebulized from a custom-built atomizer

27 and sampled into the Q-ACSM and a condensation particle counter (CPC, TSI model 3772)

Atmospheric
Chemistry
and Physics
Discussions

1   calibrating ionization efficiency (IE). IE can, therefore, be determined by comparing the response

2   factors of Q-ACSM to the mass calculated with the known particle size and the number concentration

3   from CPC.

4   Ozone (O_3) was measured by a Thermo Scientific Model 49i ozone analyzer, CO by a Thermo

5   Scientific Model 48i carbon monoxide analyzer, SO_2 by an Ecotech EC 9850 sulfur dioxide analyzer,

6   and NO_2 by a Thermo Scientific Model 42i NO-NO_2-NOx analyzer. The meteorological data,

7   including temperature, relative humidity (RH), precipitation, wind speed and wind direction, were

8   measured by an automatic weather station (MAWS201, Vaisala, Vantaa, Finland) and a wind sensor

9   (Vaisala Model QMW101-M2).

10 **2.3 Data analysis**

11 **2.3.1 Q-ACSM data analysis**

12 The mass concentrations and composition of NR-PM_1 were analyzed with the standard Q-ACSM data

13 analysis software written in Igor Pro (WaveMetrics, Inc., OR, USA). Standard relative ionization

14 efficiencies (RIEs) were used for organics, nitrate and chloride (i.e., 1.4 for organics, 1.1 for nitrate

15 and 1.3 for chloride) (Ng et al., 2011a) and RIEs for ammonium (6.0) and sulfate (1.2) were derived

16 from the IE calibrations. The particle collection efficiency (CE) was applied to correct for the particle

17 loss at the vaporizer due to particle bounce, which is influenced by aerosol acidity, composition, and

18 the aerosol water content. Given that aerosol was dried before entering into Q-ACSM and that

19 ammonium nitrate mass fraction (ANMF) during the observation period was lower than 0.4, the

20 composition dependent CE was estimated following the method described in Middlebrook et al.

21 (2012).

22 **2.3.2 The Multilinear Engine (ME-2)**

23 PMF is a bilinear receptor model that represents an input data matrix as a linear combination of a set

24 of factor profiles and their time-dependent concentrations (Paatero and Tapper, 1994). Factors

25 typically correspond to unique sources and/or processes. This allows for a quantitative apportionment

26 of bulk mass spectral time series into several factors through the minimization of a quantity Q, which

Atmospheric
Chemistry
and Physics
Discussions

1   is the sum of the squares of the error-weighted residuals of the model. The PMF-AMS/ACSM

2   analyses have been widely used for apportioning the sources of organic aerosol. However, in

3   conventional PMF analyses, rotational ambiguity with limited rotational controls can lead to unclear

4   factor resolution, especially in China where the emission sources are very complex and covariant

5   during haze events. In contrast, the multi-linear engine (ME-2), used in this study, enables efficient

6   exploration of the entire solution space and can direct the apportionment towards an environmentally-

7   meaningful solution through the constraints of a subset of priori factor profiles or time series using the

8   a value approach (Canonaco et al., 2013). The a value can vary between 0 and 1. An a value of 0.1

9   accounts for maximum $\pm$ 10% variability of each m/z signal of the final solution spectra that may

10   differ from the anchor, implying that some m/z signals might increase while some might decrease.

11   The source finder (SoFi, Canonaco et al., 2013) tool version 4.9 for Igor Pro was used for ME-2 input

12   preparation and result analysis. The number of factors resolved is determined by the user and the

13   solutions of the model are not mathematically unique due to rotational ambiguity. It is, therefore,

14   critical to study other parameters, e.g., the chemical fingerprint of the factor profiles, diurnal cycles,

15   and time series of factors and external measurements, to support factor identification and

16   interpretation (Canonaco et al., 2013; Crippa et al., 2014, Elser et al., 2016b).

17   **3 Results and discussion**

18   **3.1 Concentration and chemical composition of NR-PM$_1$**

19   Fig. 1 shows the time series of NR-PM$_1$ species, trace gases and meteorological conditions during the

20   entire measurement period. The measured mass concentrations of NR-PM$_1$ for the entire campaign

21   period ranged from a few μg m^{-3} to 508.4 μg m^{-3}, with an average of 178 $\pm$ 101 μg m^{-3}. That was

22   much higher than the wintertime/summertime concentrations measured in many other cities (see

23   Table 1). The mass concentration of NR-PM$_1$ correlated strongly with that of PM$_{2.5}$ (R^2 = 0.76) with a

24   regression slope of 0.72, indicating that NR-PM$_1$ represents a majority of PM$_{2.5}$ mass. The NR-PM$_1$

25   concentrations exceeded the Chinese PM$_{2.5}$ limit of 75 μg m^{-3} for 90% of days during the

26   measurement period, showing the severity of particulate air pollution at Shijiazhuang.

Atmospheric
Chemistry
and Physics
Discussions

1   Similar to measurements at other urban sites, OA was the dominant fraction of NR-PM$_1$, with an

2   average of 50% (31-80%), followed by 21% of sulfate (4-36%), 12% of nitrate (2-26%), 11% of

3   ammonium (4-21%) and 6% of chloride (2-20%). The dominant contribution of organics in NR-PM$_1$

4   is also consistent with measurements from other urban sites in the BTH region during winter heating

5   seasons (see Table 1). Sulfate was the second largest contributor to NR-PM$_1$. The large fraction of

6   sulfate was likely associated with the large consumption of coal in Hebei province, i.e., 296 million

7   tons in 2014 were used in coal-fired power plants and steel industry (producing ∼11% of global steel

8   output in 2014). The enhancement of chloride fraction from >1-4% in other Chinese cities in summer

9   (see Table 1) to 6% in Shijiazhuang in winter (within the range of >2-7% in other Chinese cities in

10   winter, see Table 1) can be attributed to the substantial emissions from coal and/or biomass burning

11   activities.

12   Fig. 2a shows the diurnal variations of NR-PM$_1$ components, which were affected by the evolution of

13   the planetary boundary layer (PBL) height that governed the vertical dispersion of pollutants and by

14   the diurnal cycle of the emissions and atmospheric processes. The concentrations of pollutants

15   increased at night as a result of enhanced emissions from residential heating (in particular, for

16   organics and chloride) and a progressively shallower PBL. During daytime the PBL height was

17   developed by solar radiation and thus the pollutants became diluted resulting in the decrease of

18   organics, sulfate, ammonium and chloride in the afternoon. In contrast, the concentrations of nitrate

19   increased after sunrise but then kept rather constant throughout the afternoon, suggesting a strong

20   source or production of nitrate which offsets the dilution from PBL development. To minimize the

21   effects from PBL heights, data were normalized by ΔCO. CO is often used as an emission tracer to

22   account for dilution on timescales of hours to days because of its relatively long life time against the

23   oxidation by OH radicals (approximately one month) (Decarlo et al., 2010). After offsetting the PBL

24   dilution effect, sulfate, nitrate and ammonium showed clear increases from 7:00 to 15:00 (Fig. 2c),

25   indicating efficient daytime production of these secondary inorganic species. It should be noted that

26   the increase of nitrate (about 2 times, from ∼6 µg m^{-3} ppm^{-1} to ∼12 µg m^{-3} ppm^{-1}) is slightly larger

27   than that of sulfate (about 1.6 times, from ∼11 µg m^{-3} ppm^{-1} to ∼17.5 µg m^{-3} ppm^{-1}), indicating more

28   efficient photochemical production of nitrate than sulfate, given that the loss rate of sulfate could not

Atmospheric
Chemistry
and Physics
Discussions

1   be higher than that of nitrate as nitric acid is semi-volatile and may be further lost by evaporation.

2   Also, the continuous increase of organics after sunrise suggested efficient photochemical production

3   of secondary organic aerosol (SOA).

4   **3.2 Sources of organic aerosol**

5   From the PMF analysis, we first examined a range of solutions with 3 to 8 factors. The solution that

6   best represents the data is the 5-factor solution (Fig. S1). The solutions with factor numbers more than

7   5 provide no new meaningful factors (see Fig. S2 and more details in the supplementary material).

8   Although the 5-factor solution can reasonably represent the data, HOA is still mixed with BBOA

9   because the HOA profile contains higher than expected contribution from m/z 60. In addition, COA

10   contains no signal at m/z 44, which might indicate a suboptimal splitting between the contributing

11   sources. To better separate HOA from BBOA, we constrained the HOA profile from Ng et al (2011b),

12   which is an average profile over 15 cities from China, Japan, Europe and the United States. Although

13   gasoline vehicles dominate in China while diesel vehicles dominate in Europe, HOA mass spectra do

14   not show significant variability when compared to different sites in China and Europe (Ng et al.,

15   2011b; Reyes et al., 2016; Bozzetti et al., 2017), indicating that traffic emissions from different types

16   of vehicles have similar profiles. To avoid the influences of other sources on COA, the COA profile

17   from Paris (Crippa et al., 2013) was used as a constraint because high similarities were found between

18   the COA profile from Paris and four COA profiles from different types of Chinese cooking activities

19   (He et al., 2010; Crippa et al., 2013). However, the constraint on HOA and COA profiles still seems

20   to sub-optimally resolve the apportionment of BBOA from CCOA, as one unconstrained factor

21   contains high contributions from both m/z 60 and PAH-related m/z's (m/z 77, 91 and 115, as shown in

22   Fig. S3) which indicate the mixing between BBOA and CCOA. To separate BBOA and CCOA, we

23   constrained BBOA using the average of BBOA profiles from the 5-factor unconstrained PMF

24   solutions.

25   To explore the solution space, a value of 0-0.5 with an interval of 0.1 was used to constrain both the

26   HOA and COA reference profiles from literature while BBOA was constrained with a value of 0

27   because the BBOA profile was resolved from unconstrained PMF solution which is not expected to

Atmospheric
Chemistry
and Physics
Discussions

1   vary significantly. 36 possible results were obtained by limiting a range of *a* values. Three criteria for

2   optimizing OA source appointment are as follows:

3   (1) *The diurnal pattern of COA*. The diurnal cycle of COA should have higher concentrations

4   during mealtime.

5   (2) *Minimization of m/z 60 in HOA*. The upper limit of m/z 60 in the HOA profile is 0.006, which

6   is the maximal fractional contribution derived from multiple ambient data sets in different

7   regions (mean + 2σ) (Ng et al., 2011b).

8   (3) *The rationality of unconstrained factors*. OOA should have abundant signal at *m/z* 44 and

9   contain much lower signals at PAH-related ion peaks compared to CCOA.

10   Nine solutions match the criteria above. The final time series and mass spectra are therefore the

11   averages of these 9 solutions. The diurnal variations of mass concentrations of the OA factors and

12   their PBL-corrected results are shown in Fig. 2b and d, respectively. The mass spectra and time series

13   of the OA factors and their correlation with external tracers are shown in Fig. 3. The relative

14   contributions of each OA source to the *m/z*'s are shown in Fig. S4. Potential source contribution

15   function (PSCF) analysis was also performed and the result is shown in Fig. S5.

16   OOA is characterized by high signals at *m/z* 44 (CO_2^+) and *m/z* 43 ($C_3H_7^+$ or $C_2H_3O^+$). OOA accounts

17   for 85% of *m/z* 44 signal, much higher than other OA sources. The time series of OOA is highly

18   correlated with that of sulfate (R^2=0.70), nitrate (R^2=0.75) and ammonium (R^2=0.76), confirming the

19   secondary nature of this factor. The diurnal cycle of OOA shows an increase from 7:00 to 11:00,

20   followed by a decrease in the afternoon due to the PBL evolution effect. After normalizing the PBL

21   effect, OOA increased continuously from 7:00 to 15:00, indicating the importance of photochemical

22   oxidation. This diurnal feature together with the PSCF results indicated that a large fraction of OOA

23   was produced locally and/or produced from the highly populated and industrialized surrounding areas,

24   consistent with the sulfate production discussed below.

25   The mass spectrum of CCOA is featured by prominent contributions of unsaturated hydrocarbons,

26   particularly PAH-related ion peaks (e.g., 77, 91, and 115). The CCOA profile shows a weaker signal

Atmospheric
Chemistry
and Physics
Discussions

1   at m/z 44 than that observed in Beijing (Hu et al., 2016a) and Lanzhou (Xu et al., 2016). This

2   difference can be caused by the difference in coal types, burning conditions and aging processes

3   (Zhou et al., 2016). CCOA accounts for 42-66% of PAH-related ion peaks, much higher than those in

4   other OA sources. This result suggested that the major source of PAHs was coal combustion in

5   wintertime Shijiazhuang. The average mass concentration of CCOA was 23.2 μg m^{-3}, which is higher

6   than that in Xi'an (10.1 μg m^{-3}) but is similar to that in Beijing (23.5 μg m^{-3}) observed in the same

7   winter (Elser et al., 2016a). CCOA showed distinct diurnal variations with low concentration down to

8   12.6 μg m^{-3} during the day and high concentration up to 37.6 μg m^{-3} at night, corresponding to 19%

9   and 35% of OA, respectively. The elevated CCOA concentrations at night suggested a large emission

10   from residential heating activities using coal as the fuel compounded by the shallow PBL. The

11   average contribution of CCOA to the total OA was 27%, which is consistent with studies in Beijing

12   and Handan (~160 km south to Shijiazhuang) where CCOA was found to be the dominant primary

13   OA (Elser et al., 2016a; Sun et al., 2016; Li et al., 2017). Given this large fraction of OA from coal

14   combustion, mitigating residential coal combustion is therefore of significant importance for

15   improving air quality in the BTH regions.

16   The BBOA mass spectrum is featured by prominent m/z 60 (mainly $C_2H_4O_2^+$) and 73 (mainly

17   $C_3H_5O_2^+$) signals (He et al., 2010). These two ions ($C_2H_4O_2^+$ and $C_3H_5O_2^+$) are fragments of

18   anhydrous sugars produced from the incomplete combustion and pyrolysis of cellulose and

19   hemicelluloses (Alfarra et al., 2007; Lanz et al., 2007; Mohr et al., 2009). Consistently, BBOA

20   accounts for 50% of m/z 60 and 56% of m/z 73, much higher than those in other sources. In addition,

21   BBOA accounts for 9-27% of the PAH-related m/z's (i.e., m/z 77, 91 and 115), lower than that in

22   CCOA but higher than those in other primary OA sources. This suggested that BBOA was also an

23   important PAH source in wintertime Shijiazhuang. A high correlation was found between the time

24   series of BBOA and that of chloride (R^2=0.75), the latter of which was suggested to be one of the

25   tracers of biomass burning. BBOA on average accounted for 17% of OA, which is higher than those

26   (9-12%) observed in Beijing during wintertime heating seasons (Elser et al., 2016a; Hu et al., 2016a;

27   Sun et al., 2016). The higher BBOA contribution in wintertime Shijiazhuang is likely associated with

1   widespread use of wood and crop residuals for heating and cooking in Shijiazhuang and surrounding

2   areas, as supported by the PSCF results (Fig. S5).

3   The COA profile is characterized by a high *m/z* 55/57 ratio of 2.7, much higher than that in non-

4   cooking POA (0.6-1.1) but within the range of 2.2-2.8 in COA profiles reported by Mohr et al.

5   (2012). COA shows a clear diurnal cycle with distinct peaks at lunch (between 11:00-13:00 local

6   time, LT) and dinner (between 19:00-21:00 LT) times. A small peak was also observed in the

7   morning between 06:00 and 07:00 LT, consistent with the breakfast time. COA on average accounted

8   for 16% of total OA with the highest contribution of 24% during dinner time.

9   The HOA mass spectrum is dominated by hydrocarbon ion series of $[C_nH_{2n+1}]^+$ and $[C_nH_{2n-1}]^+$

10 (Canagaratna et al., 2004; Mohr et al., 2009). The diurnal variation of HOA is featured by high

11 concentration at night, likely due to enhanced truck emissions (only allowed to drive on road from

12 23:00 to 6:00 LT) and shallow PBL at night. Similar diurnal cycles were found in wintertime Beijing

13 and Xi'an (Sun et al., 2016; Elser et al, 2016a). HOA, on average, accounted for 13% of total OA for

14 the entire observation period, which was higher than that in Beijing (9-10%) but lower than that in

15 Xi'an (15%) measured in the same winter (Elser et al., 2016a; Sun et al., 2016).

16 **3.3 Chemical nature and sources at different PM levels**

17 Fig. 4 shows the mass fractions of NR-PM$_1$ species and OA sources on reference days and extremely

18 polluted days. Here, the days with NR-PM$_1$ daily average mass concentration higher than the 75th

19 percentile (i.e., ≥238 µg m^{-3}) are denoted as the extremely polluted days and the rest of days as

20 reference days. The average concentration of NR-PM$_1$ was 310 µg m^{-3} during extremely polluted

21 days, about 2 times higher than that during reference days (162 µg m^{-3}). The average concentration of

22 secondary inorganic aerosol was 65 µg m^{-3} (40% of NR-PM$_1$ mass) during reference days and

23 increased to 143 µg m^{-3} (46% of NR-PM$_1$ mass) during extremely polluted days. Secondary organic

24 aerosol also increased from 19 µg m^{-3} (22% of OA) during reference days to 40 µg m^{-3} (26% of OA)

25 during extremely polluted days. The enhanced mass concentrations (~2 times) of both secondary

26 inorganic aerosol and secondary organic aerosol during extremely pollution days suggested strong

27 secondary aerosol production during pollution events. Such enhancement was likely compounded by

Atmospheric
Chemistry
and Physics
Discussions

1 stagnant weather conditions (e.g., average wind speed was 0.9 m s^{-1}) and high RH of 69.4% which

2 facilitated the production and accumulation of secondary aerosol. Note that it was already very

3 polluted during the reference days with an average concentration of NR-PM$_1$ of 162 µg m^{-3}, which

4 may explain the relatively small increase in fractional contribution of secondary aerosol from

5 reference days to extremely polluted days.

6 Fig. 5a and b show the factors driving the pollution events by binning the fractional contribution of

7 each chemical species and OA source to total NR-PM$_1$ and OA mass, respectively. The data clearly

8 show that high pollution events are characterized by an increasing secondary fraction, reaching ~55%

9 at the highest NR-PM$_1$ mass bin (300-360 µg m^{-3}). In particular, from the lowest NR-PM$_1$ bin to the

10 highest NR-PM$_1$ bin, the fractional contribution increases from 14% to 25% for sulfate in NR-PM$_1$

11 and from 18% to 25% for OOA in OA, demonstrating the importance of secondary aerosol formation

12 in driving particulate air pollution (Huang et al., 2014; Elser et al., 2016; Wang et al., 2017). To

13 investigate the oxidation degree of sulfur at different NR-PM$_1$ mass, the sulfur oxidation ratio (F_{SO4})

14 was calculated according to Eq. (1)

$$F_{SO_4^{2-}} = \frac{n\left[SO_4^{2-}\right]}{n\left[SO_4^{2-}\right] + n[SO_2]} \tag{1}$$

15

16 where n is the molar concentration. As can be seen from Fig. 6, F_{SO4} shows a clear increase trend with

17 NR-PM$_1$ mass, increasing from 0.08 in the lowest mass bin to 0.21 in the highest mass bin. However,

18 the highest F_{SO4} value is still much lower than that reported in previous studies, e.g., 0.62 in Xi'an

19 (Elser et al., 2016), suggesting low atmospheric oxidative capacity during the measurement period in

20 Shijiazhuang. This may also explain the relatively low OOA fraction (see Fig. 5b).

21 **3.4 Evolution of aerosol composition and sources at different RH levels**

22 Fig. 7a and b show the mass concentrations of the NR-PM$_1$ species and of the OA sources as a

23 function of RH, with RH bins of 10% increments. The absolute mass concentrations of secondary

24 inorganic species increased as RH increased from <60% to 90%, while chloride showed a decreasing

25 trend. Among the OA sources, OOA was significantly enhanced with RH increasing from <60% to

Atmospheric
Chemistry
and Physics
Discussions

1   90%, while other OA sources did not show a clear trend. As RH increased gradually with the decrease

2   of wind speed (Fig. 6a), the development of stagnant weather conditions (including a shallower PBL)

3   promoted both the accumulation of pollutants and the formation of secondary aerosol (Tie et al.,

4   2016). To minimize the effects from PBL variations, the NR-PM$_1$ species and OA fractions were

5   normalized by the sum of the POA, as a surrogate of secondary aerosol precursors. The resulting

6   ratios were further normalized by the values at the first RH bin (<60%) for better visualization. As

7   shown in Fig. 7c, when RH increased from <60% to >90%, the normalized sulfate increased by a

8   factor of ∼2.5, suggesting the importance of aqueous-phase SO$_2$ oxidation in the formation of sulfate

9   at high RH. The enhancements for nitrate and ammonium were slightly lower (∼1.5) compared to that

10   sulfate, because NH$_4$NO$_3$ is thermal lability and its gas-particle partitioning is affected by both

11   temperature and RH. The importance of aqueous-phase chemistry is further supported by the increase

12   of F_{SO4} as a function of RH (Fig. 6b). At RH <60%, F_{SO4} was rather constant, with an average of 0.09,

13   indicating a low sulfur oxidation degree. At RH >60%, F_{SO4} increased rapidly with the increase of

14   RH, reaching a maximal average of 0.18 at the last RH bin (90-100%). Note that the sulfur oxidation

15   degree at high RH (>60%) was much lower compared to those measured in Xi'an during the same

16   winter (average F_{SO4} 0.62 at RH=90-100%, Elser et al., 2016a). The low sulfur oxidation degree

17   observed in Shijiazhuang (i.e., >80% of sulfur is still not oxidized) indicated insufficient atmospheric

18   processing and also suggested a large fraction of pollutants in Shijiazhuang was likely emitted locally

19   and/or transported from the heavily populated and industrialized surrounding areas. With a longer

20   atmospheric processing time in the downwind region, e.g., Beijing, higher secondary aerosol fractions

21   are expected, as observed in previous studies (e.g., Huang et al., 2014). Similar to sulfate, the

22   normalized OOA increased by a factor of ∼3 when RH increased from <60% to 90-100% (Fig. 7d).

23   The mass fraction of OOA increased from 29% to 41% when RH increased from 70% to 100%, while

24   POA contribution decreased correspondingly from 71% to 59% (Fig. 6d). These results support the

25   above discussion that aqueous-phase chemistry also plays an important role in the formation of OOA

26   under high RH conditions during haze pollution episodes.

27   **3.5 Primary emissions versus secondary formation**

Atmospheric
Chemistry
and Physics
Discussions

1   Frequent changes between clean and polluted episodes were observed in this study. To get a better

2   insight into aerosol sources and atmospheric processes, 4 clean periods (C1-C4) with daily average

3   mass concentration of NR-PM$_1$ lower than the 25th percentile, 6 high-RH (>80%) polluted episodes

4   (H1-H6) and 4 low-RH (<60%) polluted episodes (L1-L4) with daily average mass concentration of

5   NR-PM$_1$ higher than the 75th percentile were selected for further analysis. As shown in the Fig. 8, the

6   chemical composition and sources differed during different episodes. The contributions of organics

7   showed a decreasing trend, from 54-64% during C1-C4 to 49-58% during L1-L4, and to 35-44%

8   during H1-H6, while the corresponding contributions of secondary inorganic species increased. This

9   indicated a notable production and accumulation of secondary inorganic aerosol during severe haze

10   pollution events. For example, the mass fraction of sulfate in NR-PM$_1$ was much higher during high

11   RH pollution events (H1-H6, 27-30%) compared to those during low RH pollution events (L1-L4, 11-

12   18%) and clean events (C1-C4, 11-17%). OOA also showed a much higher contribution to OA during

13   high RH pollution events (H1-H6, 29-50%) than during low RH pollution events (L1-L3, 17-26%)

14   and clean events (C1-C4, 10-34%). Interestingly, when comparing high RH and low RH pollution

15   events of similar PM levels (Fig. 8), secondary inorganic species and OOA dominated the particulate

16   pollution at high RH pollution events, similar to previous studies (e.g., Wang et al., 2017), while POA

17   dominated the particulate pollution at low RH and under stagnant conditions. These results highlight

18   the importance of meteorological conditions in driving particulate pollution.

19   Fig. 9 shows the evolution of aerosol species in two cases of different RH levels. The first case had

20   average RH <50% from 20-24 Jan (C2 and L3 episodes). The high wind speed (>6 m s^{-1}) from the

21   northwest before the L3 episode led to a significant reduction of air pollutants (the C3 episode, a

22   clean-up period). When the wind direction switched from northwest to 90°-270° sector and the wind

23   speed decreased to <3 m s^{-1}, the measured pollutants (except O$_3$ which was reacted out by increasing

24   NO emissions) started to build up. Specifically, NR-PM$_1$ showed a dramatic increase by a factor of 19

25   over the first 11 hours (from 20 Jan 16:00 to 21 Jan 3:00 LT) from 12 to 233 μg m^{-3}. In this process

26   POA contributed to an average 69% of NR-PM$_1$ mass. The other three processes were also

27   characterized by a rapid increase of NR-PM$_1$ mass (39-50 μg m^{-3} h^{-1}) and high contribution of POA,

28   i.e., from 22 Jan 0:00-22 Jan 3:00, 22 Jan 16:00-22 Jan 20:00, and 23 Jan 12:00-23 Jan 19:00. Such

Atmospheric
Chemistry
and Physics
Discussions

1   rapid increases in NR-PM$_1$ mass under low RH were associated with stagnant weather conditions

2   (e.g., low wind speed) which promoted the accumulation of pollutants. The second case had average

3   RH >80% from 5-8 Feb (H3 and H4 episodes). In this case, the wind speed was low (<3 m s^{-1})

4   throughout the 4-day period. Under this very stagnant weather condition, POA accumulated

5   continuously (Fig. 9). However, different from the low-RH case, the concentration of secondary

6   species also showed continuous increases in this high-RH case. The enhancement of secondary

7   aerosol formation was likely driven by aqueous-phase chemistry at high RH level (Elser et al., 2016;

8   Wang et al., 2017) and the accumulation of pollutants under stagnant weather conditions (Tie et al.,

9   2017) which further promoted the formation of secondary species.

10 **4 Conclusions**

11   A Quadrupole Aerosol Chemical Speciation Monitor (Q-ACSM) was deployed in Shijiazhuang from

12   11 January to 18 February 2014 to investigate the chemical nature, sources and atmospheric processes

13   of fine particles in this heavily polluted city. The average mass concentration of NR-PM$_1$ was 178 ±

14   101 µg m^{-3}, much higher than the wintertime concentrations measured in many other cities. Organics

15   were the dominant composition (50%), followed by sulfate (21%), nitrate (12%), ammonium (11%)

16   and chloride (6%). As for the sources of OA, OOA (27%) and CCOA (27%) were on average the

17   most abundant sources, followed by BBOA (17%), COA (16%) and HOA (13%). The mass fractions

18   of secondary inorganic species and SOA increased with the increase of NR-PM$_1$ mass, suggesting the

19   importance of secondary formation in driving PM pollution. However, the low sulfur oxidation degree

20   and low OOA fraction indicated insufficient atmospheric oxidation capacity. Together with the

21   diurnal variations and PSCF results, these observations suggested that a large fraction of pollutants in

22   Shijiazhuang was most likely produced locally and/or transported from the heavily populated and

23   industrialized surrounding areas without sufficient atmospheric aging. Two different regimes were

24   found to be responsible for the high PM pollution in Shijiazhuang. At low RH under stagnant weather

25   conditions, the accumulation of primary emissions was the main culprit. In contrast, at high RH, the

26   enhanced formation of secondary aerosol through aqueous-phase chemistry was the main culprit. To

27   conclude, we found that in this highly polluted city in North China, (1) secondary formation is

Atmospheric
Chemistry
and Physics
Discussions
Open Access
EGU

1   important in high-PM episodes, (2) primary emissions are still important on an average basis, and (3)

2   meteorological conditions play an important part in pollutant accumulation and transformation. The

3   findings from this study thus suggest that (a) there are still opportunities for air pollution mitigation

4   by controlling direct emissions such as coal combustion, and (b) control on precursors (e.g., NO_x,

5   SO_2, and VOCs) for secondary formation, especially during high-PM episodes with unfavorable

6   meteorological conditions, can ease the situation substantially.

7   **5 Acknowledgement**

10

11   **References**

12   Alfarra, M. R., Prévôt, A. S. H., Szidat, S., Sandradewi, J.,Weimer, S., Schreiber, D., Mohr, M., and

13   Baltensperger, U.: Identification of the mass spectral signature of organic aerosols from wood burning

14   emissions, Environ. Sci. Technol., 41, 5770–5777, 2007.

15   Bozzetti, C., El Haddad, I., Salameh, D., Daellenbach, K. R., Fermo, P., Gonzalez, R., Minguillón, M.

16   C., Iinuma, Y., Poulain, L., Müller, E., Slowik, J. G., Jaffrezo, J.-L., Baltensperger, U., Marchand, N.,

17   and Prévôt, A. S. H.: Organic aerosol source apportionment by offline-AMS over a full year in

18   Marseille, Atmos. Chem. Phys. Discuss., 17, 8247-8268, 2017.

19   Bressi, M., Cavalli, F., Belis, C. A., Putaud, J.-P., Fröhlich, R., Martins dos Santos, S., Petralia, E.,

20   Prévôt, A. S. H., Berico, M., Malaguti, A., and Canonaco, F.: Variations in the chemical composition

21   of the submicron aerosol and in the sources of the organic fraction at a regional background site of the

22   Po Valley (Italy), Atmos. Chem. Phys., 16, 12875-12896, https://doi.org/10.5194/acp-16-12875-2016,

23   2016.

24   Canagaratna, M. R., Jayne, J. T., Ghertner, D. A., Herndon, S., Shi, Q., Jimenez, J. L., Silva, P. J.,

25   Williams, P., Lanni, T., Drewnick, F., Demerjian, K. L., Kolb, C. E., Worsnop, D. R.: Chase studies

26   of particulate emissions from in-use New York City vehicles, Aerosol Sci. Tech. 38, 555-573, 2004.

Atmospheric
Chemistry
and Physics
Discussions

1 Canonaco, F., Crippa, M., Slowik, J. G., Baltensperger, U., and Prévôt, A. S. H.: SoFi, an IGOR

2 based interface for the efficient use of the generalized multilinear engine (ME-2) for the source

3 apportionment: ME-2 application to aerosol mass spectrometer data, Atmos. Meas. Tech., 6, 3649–

4 3661, doi:10.5194/amt-6-3649-2013, 2013.

5 Canonaco, F., Slowik, J. G., Baltensperger, U., and Prévôt, A. S. H.: Seasonal differences in

6 oxygenated organic aerosol composition: implications for emissions sources and factor analysis,

7 Atmos. Chem. Phys., 15, 6993-7002, doi:10.5194/acp-15-6993-2015, 2015.

8 Chen, D. S., Cheng, S. Y., Liu, L., Chen, T., Guo, X. R.: An integrated MM5-CMAQ modeling

9 approach for assessing trans-boundary PM10 contribution to the host city of 2008 Olympic summer

10 games-Beijing, China, Atmospheric Environment, 41, 1237-1250, 2007.

11 Crippa, M., DeCarlo, P. F., Slowik, J. G., Mohr, C., Heringa, M. F., Chirico, R., Poulain, L., Freutel,

12 F., Sciare, J., Cozic, J., Di Marco, C. F., Elsasser, M., Nicolas, J. B., Marchand, N., Abidi, E.,

13 Wiedensohler, A., Drewnick, F., Schneider, J., Borrmann, S., Nemitz, E., Zimmermann, R., Jaffrezo,

14 J.-L., Prévôt, A. S. H., and Baltensperger, U.: Wintertime aerosol chemical composition and source

15 apportionment of the organic fraction in the metropolitan area of Paris, Atmos. Chem. Phys., 13, 961-

16 981, doi:10.5194/acp-13-961-2013, 2013.

17 Crippa, M., Canonaco, F., Lanz, V. A., Äijälä, M., Allan, J. D., Carbone, S., Capes, G., Ceburnis, D.,

18 Dall'Osto, M., Day, D. A., DeCarlo, P. F., Ehn, M., Eriksson, A., Freney, E., Hildebrandt Ruiz, L.,

19 Hillamo, R., Jimenez, J. L., Junninen, H., Kiendler-Scharr, A., Kortelainen, A.-M., Kulmala, M.,

20 Laaksonen, A., Mensah, A. A., Mohr, C., Nemitz, E., O'Dowd, C., Ovadnevaite, J., Pandis, S. N.,

21 Petäjä, T., Poulain, L., Saarikoski, S., Sellegri, K., Swietlicki, E., Tiitta, P., Worsnop, D. R.,

22 Baltensperger, U., and Prévôt, A. S. H.: Organic aerosol components derived from 25 AMS data sets

23 across Europe using a consistent ME-2 based source apportionment approach, Atmos. Chem. Phys.,

24 14, 6159– 6176, doi:10.5194/acp-14-6159-2014, 2014.

25 Decarlo, P. F., Ulbrich, I. M., Crounse, J., De Foy, B., Dunlea, E. J., Aiken, A. C., Knapp, D.,

26 Weinheimer, A. J., Campos, T., Wennberg, P. O., Jimenez, J. L.: Investigation of the sources and

Atmospheric
Chemistry
and Physics
Discussions

1 processing of organic aerosol over the Central Mexican Plateau from aircraft measurements during

2 MILAGRO, Atmos. Chem. Phys., 10, 5257-5280, doi:10.5194/acp-10-5257-2010, 2010

3 Elser, M., Huang, R.-J., Wolf, R., Slowik, J. G., Wang, Q., Canonaco, F., Li, G., Bozzetti, C.,

4 Daellenbach, K. R., Huang, Y., Zhang, R., Li, Z., Cao, J., Baltensperger, U., El-Haddad, I., and

5 Prévôt, A. S. H.: New insights into PM2.5 chemical composition and sources in two major cities in

6 China during extreme haze events using aerosol mass spectrometry, Atmos. Chem. Phys., 16, 3207-

7 3225, doi:10.5194/acp-16-3207-2016, 2016a.

8 Elser, M., Bozzetti, C., El-Haddad, I., Maasikmets, M., Teinemaa, E., Richter, R., Wolf, R., Slowik, J.

9 G., Baltensperger, U., and Prévôt, A. S. H.: Urban increments of gaseous and aerosol pollutants and

10 their sources using mobile aerosol mass spectrometry measurements, Atmos. Chem. Phys., 16, 7117-

11 7134, doi:10.5194/acp-16-7117-2016, 2016b.

12 Ervens, B., Turpin, B. J., and Weber, R. J.: Secondary organic aerosol formation in cloud droplets and

13 aqueous particles (aqSOA): a review of laboratory, field and model studies, Atmos. Chem. Phys., 11,

14 11069–11102, doi:10.5194/acp-11-11069-2011, 2011.

15 Fröhlich, R., Cubison, M. J., Slowik, J. G., Bukowiecki, N., Prévôt, A. S. H., Baltensperger, U.,

16 Schneider, J., Kimmel, J. R., Gonin, M., Rohner, U., Worsnop, D. R., and Jayne, J. T.: The ToF-

17 ACSM: a portable aerosol chemical speciation monitor with TOFMS detection, Atmos. Meas. Tech.,

18 6, 3225-3241, https://doi.org/10.5194/amt-6-3225-2013, 2013.

19 Fröhlich, R., Crenn, V., Setyan, A., Belis, C. A., Canonaco, F., Favez, O., Riffault, V., Slowik, J. G.,

20 Aas, W., Aijälä, M., Alastuey, A., Artiñano, B., Bonnaire, N., Bozzetti, C., Bressi, M., Carbone, C.,

21 Coz, E., Croteau, P. L., Cubison, M. J., Esser-Gietl, J. K., Green, D. C., Gros, V., Heikkinen, L.,

22 Herrmann, H., Jayne, J. T., Lunder, C. R., Minguillón, M. C., Mocnik, G., O'Dowd, C. D.,

23 Ovadnevaite, J., Petralia, E., Poulain, L., Priestman, M., Ripoll, A., Sarda-Estève, R., Wiedensohler,

24 A., Baltensperger, U., Sciare, J., and Prévôt, A. S. H.: ACTRIS ACSM intercomparison–Part 2:

25 Intercomparison of ME-2 organic source apportionment results from 15 individual, co-located aerosol

26 mass spectrometers, Atmos. Meas. Tech., 8, 2555–2576, doi:10.5194/amt- 8-2555-2015, 2015a.

Atmospheric
Chemistry
and Physics
Discussions

1 Fröhlich, R., Cubison, M. J., Slowik, J. G., Bukowiecki, N., Canonaco, F., Croteau, P. L., Gysel, M.,

2 Henne, S., Herrmann, E., Jayne, J. T., Steinbacher, M., Worsnop, D. R., Baltensperger, U., and

3 Prévôt, A. S. H.: Fourteen months of on-line measurements of the non-refractory submicron aerosol at

4 the Jungfraujoch (3580 m a.s.l.) – chemical composition, origins and organic aerosol sources, Atmos.

5 Chem. Phys., 15, 11373-11398, doi:10.5194/acp-15-11373-2015, 2015b.

6 Ge, X., Zhang, Q., Sun, Y. L., Ruehl, C. R., and Setyan, A.: Effect of aqueous-phase processing on

7 aerosol chemistry and size distributions in Fresno, California, during wintertime, Environmental

8 Chemistry, 9, 221–235, doi:10.1071/EN11168, 2012.

9 Guo, S., Hu, M., Wang, Z. B., Slanina, J., and Zhao, Y. L.: Size resolved aerosol water-soluble ionic

10 compositions in the summer of Beijing: implication of regional secondary formation, Atmos. Chem.

11 Phys., 10, 947–959, doi:10.5194/acp-10-947-2010, 2010.

12 He, L.-Y., Lin, Y., Huang, X.-F., Guo, S., Xue, L., Su, Q., Luan, S.- J., and Zhang, Y.-H.:

13 Characterization of high-resolution aerosol mass spectra of primary organic aerosol emissions from

14 Chinese cooking and biomass burning, Atmos. Chem. Phys., 10, 11535– 11543, doi:10.5194/acp-10-

15 11535-2010, 2010.

16 He, L.-Y., Huang, X.-F., Xue, L., Hu, M., Lin, Y., Zheng, J., Zhang, R., and Zhang, Y.-H.: Submicron

17 aerosol analysis and organic source apportionment in an urban atmosphere in Pearl River Delta of

18 China using high-resolution aerosol mass spectrometry, J. Geophys. Res., 116, D12304,

19 doi:10.1029/2010JD014566, 2011.

20 Hu, W., Hu, M., Hu, W., Jimenez, J. L., Yuan, B., Chen, W., Wang, M., Wu, Y., Chen, C., Wang, Z.,

21 Peng, J., Zeng, L., and Shao, M.: Chemical composition, sources and aging process of submicron

22 aerosols in Beijing: contrast between summer and winter, J. Geophys. Res., 121, 1955–1977,

23 doi:10.1002/2015JD024020, 2016a.

24 Hu, W., Hu, M., Hu, W.-W., Niu, H., Zheng, J., Wu, Y., Chen, W., Chen, C., Li, L., Shao, M., Xie,

25 S., and Zhang, Y.: Characterization of submicron aerosols influenced by biomass burning at a site in

Atmospheric
Chemistry
and Physics
Discussions

Open Access

EGU

1   the Sichuan Basin, southwestern China, Atmos. Chem. Phys., 16, 13213-13230, doi:10.5194/acp-16-

2   13213-2016, 2016b.

3   Huang, R. J., Zhang, Y., Bozzetti, C., Ho, K. F., Cao, J. J., Han, U., Daellenbach, K. R., Slowik, J. G.,

4   Platt, S. M., Canonaco, F., Zotter, P., Wolf, R., Pieber, S. M., Bruns, E. A., Crippa, M., Ciarelli, G.,

5   Piazzalunga, A., Schwikowski, M., Abbaszade, G., Schnelle-Kreis, J., Zimmermann, R., An, Z.,

6   Szidat, S., Baltensperger, U., El Haddad, I. and Prévôt, A. S. H.: High secondary aerosol contribution

7   to particulate pollution during haze events in China, Nature, 514, 218–222, 2014.

8   Huang, X.-F., He, L.-Y., Xue, L., Sun, T.-L., Zeng, L.-W., Gong, Z.-H., Hu, M., and Zhu, T.: Highly

9   time-resolved chemical characterization of atmospheric fine particles during 2010 Shanghai World

10   Expo, Atmos. Chem. Phys., 12, 4897-4907, doi:10.5194/acp-12-4897-2012, 2012.

11   Huang, X.-F., Xue, L., Tian, X.-D., Shao, W.-W., Sun, T.-L., Gong, Z.-H., Ju, W.-W., Jiang, B., Hu,

12   M., and He, L.-Y.: Highly time-resolved carbonaceous aerosol characterization in yangtze river delta

13   of china: Composition, mixing state and secondary formation, Atmos. Environ., 64, 200–207,

14   doi:10.1016/j.atmosenv.2012.09.059, 2013.

15   Jiang, Q., Sun, Y. L., Wang, Z., and Yin, Y.: Aerosol composition and sources during the Chinese

16   Spring Festival: fireworks, secondary aerosol, and holiday effects, Atmos. Chem. Phys., 15, 6023–

17   6034, doi:10.5194/acp-15-6023-2015, 2015.

18   Jimenez, J. L., Canagaratna, M. R., Donahue, N. M., Prévôt, A. S. H., Zhang, Q., Kroll, J. H.,

19   DeCarlo, P. F., Allan, J. D., Coe, H., Ng, N. L., Aiken, A. C., Docherty, K. S., Ulbrich, I. M.,

20   Grieshop, A. P., Robinson, A. L., Duplissy, J., Smith, J. D., Wilson, K. R., Lanz, V. A., Hueglin, C.,

21   Sun, Y. L., Tian, J., Laaksonen, A., Raatikainen, T., Rautiainen, J., Vaattovaara, P., Ehn, M.,

22   Kulmala, M., Tomlinson, J. M., Collins, D. R., Cubison, M. J., E, Dunlea, J., Huffman, J. A., Onasch,

23   T. B., Alfarra, M. R., Williams, P. I., Bower, K., Kondo, Y., Schneider, J., Drewnick, F., Borrmann,

24   S., Weimer, S., Demerjian, K., Salcedo, D., Cottrell, L., Griffin, R., Takami, A., Miyoshi, T.,

25   Hatakeyama, S., Shimono, A., Sun, J. Y., Zhang, Y. M., Dzepina, K., Kimmel, J. R., Sueper, D.,

26   Jayne, J. T., Herndon, S. C., Trimborn, A. M., Williams, L. R., Wood, E. C., Middlebrook, A. M.,

Atmospheric
Chemistry
and Physics
Discussions

1   Kolb, C. E., Baltensperger, U., and Worsnop, D. R.: Evolution of organic aerosols in the atmosphere,

2   Science, 326, 1525–1529, 2009.

3   Lang, J.L., Cheng, S.Y., Li, J.B., Chen, D.S., Zhou, Y., Wei, X., Han, L.H., and Wang, H.Y.: A

4   monitoring and modeling study to investigate regional transport and characteristics of PM2.5

5   pollution, Aerosol Air Qual. Res., 13, 943–956, 2013.

6   Lanz, V. A., Alfarra, M. R., Baltensperger, U., Buchmann, B., Hueglin, C., and Prévôt, A. S. H.:

7   Source apportionment of submicron organic aerosols at an urban site by factor analytical modelling of

8   aerosol mass spectra, Atmos. Chem. Phys., 7, 1503-1522, doi:10.5194/acp-7-1503-2007, 2007.

9   Lelieveld, J., Evans, J. S., Fnais, M., Giannadaki, D., and Pozzer, A.: The contribution of outdoor air

10   pollution sources to premature mortality on a global scale, Nature, 525, 367-371, 2015.

11   Li, H., Zhang, Q., Zhang, Q., Chen, C., Wang, L., Wei, Z., Zhou, S., Parworth, C., Zheng, B.,

12   Canonaco, F., Prévôt, A. S. H., Chen, P., Zhang, H., Wallington, T. J., and He, K.: Wintertime aerosol

13   chemistry and haze evolution in an extremely polluted city of North China Plain: significant

14   contribution from coal and biomass combustions, Atmos. Chem. Phys. , 17, 4751-4768,

15   doi:10.5194/acp-2016-1058, 2017.

16   Li, P., Yan, R., Yu, S., Wang, S., Liu, W., and Bao, H.: Reinstate regional transport of $PM_{2.5}$ as a

17   major cause of severe haze in Beijing, P. Natl. Acad. Sci., 112, E2739–E2740,

18   doi:10.1073/pnas.1502596112, 2015a.

19   Li, Y. J., Lee, B. Y. L., Yu, J. Z., Ng, N. L., and Chan, C. K.: Evaluating the degree of oxygenation of

20   organic aerosol during foggy and hazy days in Hong Kong using high-resolution time-of-flight

21   aerosol mass spectrometry (HR-ToF-AMS), Atmos. Chem. Phys., 13, 8739–8753, doi:10.5194/acp-

22   13-8739-2013, 2013

23   Li, Y. J., Lee, B. P., Su, L., Fung, J. C. H., and Chan, C. K.: Seasonal characteristics of fine

24   particulate matter (PM) based on high-resolution time-of-flight aerosol mass spectrometric (HR-ToF-

25   AMS) measurements at the HKUST Supersite in Hong Kong, Atmos. Chem. Phys., 15, 37-53,

26   doi:10.5194/acp-15-37-2015, 2015b.

Atmospheric
Chemistry
and Physics
Discussions

1 Middlebrook, A. M., Bahreini, R., Jimenez, J. L., and Canagaratna, M. R.: Evaluation of

2 Composition-Dependent Collection Efficiencies for the Aerodyne Aerosol Mass Spectrometer using

3 Field Data, Aerosol Sci. Tech., 46, 258–271, 2012.

4 Minguillón, M. C., Ripoll, A., Pérez, N., Prévôt, A. S. H., Canonaco, F., Querol, X., and Alastuey, A.:

5 Chemical characterization of submicron regional background aerosols in the western Mediterranean

6 using an Aerosol Chemical Speciation Monitor, Atmos. Chem. Phys., 15, 6379-6391,

7 doi:10.5194/acp-15-6379-2015, 2015.

8 Mohr, C., Huffman, J. A., Cubison, M. J., Aiken, A. C., Docherty, K. S., Kimmel, J. R., Ulbrich, I.

9 M., Hannigan, M., and Jimenez, J. L.: Characterization of primary organic aerosol emissions from

10 meat cooking, trash burning, and motor vehicles with High-Resolution Aerosol Mass Spectrometry

11 and comparison with ambient and chamber observations, Environ. Sci. Technol., 43, 2443–2449,

12 doi:10.1021/es8011518, 2009.

13 Mohr, C., DeCarlo, P. F., Heringa, M. F., Chirico, R., Slowik, J. G., Richter, R., Reche, C., Alastuey,

14 A., Querol, X., Seco, R., Peñuelas, J., Jiménez, J. L., Crippa, M., Zimmermann, R., Baltensperger,

15 U., and Prévôt, A. S. H.: Identification and quantification of organic aerosol from cooking and other

16 sources in Barcelona using aerosol mass spectrometer data, Atmos. Chem. Phys., 12, 1649–1665,

17 doi:10.5194/acp-12-1649-2012, 2012.

18 Ng, N. L., Canagaratna, M. R., Zhang, Q., Jimenez, J. L., Tian, J., Ulbrich, I. M., Kroll, J. H.,

19 Docherty, K. S., Chhabra, P. S., Bahreini, R., Murphy, S. M., Seinfeld, J. H., Hildebrandt, L.,

20 Donahue, N. M., DeCarlo, P. F., Lanz, V. A., Prévôt, A. S. H., Dinar, E., Rudich, Y., and Worsnop,

21 D. R.: Organic aerosol components observed in Northern Hemispheric datasets from Aerosol Mass

22 Spectrometry, Atmos. Chem. Phys., 10, 4625-4641, doi:10.5194/acp-10-4625-2010, 2010.

23 Ng, N. L., Herndon, S. C., Trimborn, A., Canagaratna, M. R., Croteau, P. L., Onasch, T. B., Sueper,

24 D.,Worsnop, D. R., Zhang, Q., Sun, Y. L., and Jayne, J. T.: An Aerosol Chemical Speciation Monitor

25 (ACSM) for Routine Monitoring of the Composition and Mass Concentrations of Ambient Aerosol,

26 Aerosol Sci. Tech., 45, 770–784, 2011a.

Atmospheric
Chemistry
and Physics
Discussions

Open Access

1 Ng, N. L., Canagaratna, M. R., Jimenez, J. L., Zhang, Q., Ulbrich, I. M., and Worsnop, D. R.: Real-
2 time methods for estimating organic component mass concentrations from aerosol mass spectrometer
3 data, Environ. Sci. Technol., 45, 910–916, 2011b.

4 Paatero, P., and Tapper, U., Positive Matrix Factorization: A Non-Negative Factor Model with
5 Optimal Utilization of Error Estimates of Data Values, Environmetrics, 5, 111–126, doi:
6 10.1002/env.3170050203, 1994.

7 Petit, J.-E., Favez, O., Sciare, J., Crenn, V., Sarda-Estève, R., Bonnaire, N., Močnik, G., Dupont, J.-
8 C., Haeffelin, M., and Leoz-Garziandia, E.: Two years of near real-time chemical composition of
9 submicron aerosols in the region of Paris using an Aerosol Chemical Speciation Monitor (ACSM) and
10 a multi-wavelength Aethalometer, Atmos. Chem. Phys., 15, 2985-3005, doi:10.5194/acp-15-2985-
11 2015, 2015.

12 Ripoll, A., Minguillón, M. C., Pey, J., Jimenez, J. L., Day, D. A., Sosedova, Y., Canonaco, F., Prévôt,
13 A. S. H., Querol, X., and Alastuey, A.: Long-term real-time chemical characterization of submicron
14 aerosols at Montsec (southern Pyrenees, 1570 m a.s.l.), Atmos. Chem. Phys., 15, 2935-2951,
15 doi:10.5194/acp-15-2935-2015, 2015.

16 Reyes-Villegas, E., Green, D. C., Priestman, M., Canonaco, F., Coe, H., Prévôt, A. S. H., and Allan, J.
17 D.: Organic aerosol source apportionment in London 2013 with ME-2: exploring the solution space
18 with annual and seasonal analysis, Atmos. Chem. Phys., 16, 15545-15559, doi:10.5194/acp-16-
19 15545-2016, 2016.

20 Schlag, P., Kiendler-Scharr, A., Blom, M. J., Canonaco, F., Henzing, J. S., Moerman, M., Prévôt, A.
21 S. H., and Holzinger, R.: Aerosol source apportionment from 1-year measurements at the CESAR
22 tower in Cabauw, the Netherlands, Atmos. Chem. Phys., 16, 8831-8847, https://doi.org/10.5194/acp-
23 16-8831-2016, 2016.

24 Schneider, J., Weimer, S., Drewnick, F., Borrmann, S., Helas, G. Gwaze, P., Schmid, O., Andreae, M.
25 O., and Kirchner, U.: Mass spectrometric analysis and aerodynamic properties of various types of

Atmospheric
Chemistry
and Physics
Discussions
Open Access
EGU

1   combustion-related   aerosol   particles,   Int.   J.   Mass   Spectrom.,   258,   37–49,

2   doi:10.1016/j.ijms.2006.07.008, 2006.

3   Sun, Y. L., Wang, Z. F., Fu, P. Q., Yang, T., Jiang, Q., Dong, H. B., Li, J., and Jia, J. J.: Aerosol

4   composition, sources and processes during wintertime in Beijing, China, Atmos. Chem. Phys., 13,

5   4577–4592, doi:10.5194/acp-13-4577-2013, 2013.

6   Sun, Y. L., Jiang, Q., Wang, Z., Fu, P., Li, J., Yang, T., and Yin, Y.: Investigation of the sources and

7   evolution processes of severe haze pollution in Beijing in January 2013, J. Geophys. Res., 119, 4380–

8   4398, doi:10.1002/2014JD021641, 2014.

9   Sun, Y. L., Wang, Z. F., Du, W., Zhang, Q., Wang, Q. Q., Fu, P. Q., Pan, X. L., Li, J., Jayne, J., and

10   Worsnop, D. R.: Long-term real-time measurements of aerosol particle composition in Beijing, China:

11   seasonal variations, meteorological effects, and source analysis, Atmos. Chem. Phys., 15, 10149-

12   10165, doi:10.5194/acp-15-10149-2015, 2015.

13   Sun, Y., Du, W., Fu, P., Wang, Q., Li, J., Ge, X., Zhang, Q., Zhu, C., Ren, L., Xu, W., Zhao, J., Han,

14   T., Worsnop, D. R., and Wang, Z.: Primary and secondary aerosols in Beijing in winter: sources,

15   variations and processes, Atmos. Chem. Phys., 16, 8309-8329, doi:10.5194/acp-16-8309-2016, 2016.

16   Tie, X., Huang, R. J., Cao, J. J., Zhang, Q., Cheng, Y. F., Su, H., Chang, D., Pöschl, U., Hoffmann,

17   T., Dusek, U., Li, G. H., Worsnop, D. R., O'Dowd, C. D.: Severe pollution in China amplified by

18   atmospheric moisture, Sci. Rep., 7: 15760, DOI:10.1038/s41598-017-15909-1, 2017

19   Ulbrich, I. M., Canagaratna, M. R., Zhang, Q., Worsnop, D. R., and Jimenez, J. L.: Interpretation of

20   organic components from Positive Matrix Factorization of aerosol mass spectrometric data, Atmos.

21   Chem. Phys., 9, 2891-2918, doi:10.5194/acp-9-2891-2009, 2009.

22   Wang, G., Zhang, R., Gomez, M.E., Yang, L., Levy Zamora, M., Hu, M., Lin, Y., Peng, J., Guo, S.,

23   Meng, J., Li, J., Cheng, C., Hu, T., Ren, Y., Wang, Y., Gao, J., Cao, J., An, Z., Zhou, W., Li, G.,

24   Wang, J., Tian, P., Marrero-Ortiz, W., Secrest, J., Du, Z., Zheng, J., Shang, D., Zeng, L., Shao, M.,

25   Wang, W., Huang, Y., Wang, Y., Zhu, Y., Li, Y., Hu, J., Pan, B., Cai, L., Cheng, Y., Ji, Y., Zhang, F.,

Atmospheric
Chemistry
and Physics
Discussions
Open Access

1   Rosenfeld, D., Liss, P.S., Duce, R.A., Kolb, C.E., and Molina, M.J., Persistent sulfate formation from
2   London fog to Chinese haze, Proc. Natl. Acad. Sci., 113, 13630-13635,2016.

3   Wang, Q, Sun Y, Jiang Q, et al. Chemical composition of aerosol particles and light extinction
4   apportionment before and during the heating season in Beijing, China, J. Geophys. Res. Atmos., 120,
5   12708-12722, 2015.

6   Wang, Y. C., Huang, R. J., Ni, H. Y., Chen, Y., Wang, Q. Y., Li, G. H., Tie, X. X., Shen, Z. X.,
7   Huang, Y., Liu, S. X., Dong, W. M., Xue, P., Frohlich, R., Canonaco, F., Elser, M., Daellenbach, K.
8   R., Bozzetti, C., El Haddad, I., Prevot, A. S. H.: Chemical composition, sources and secondary
9   processes of aerosols in Baoji city of northwest China, Atmos. Environ., 158, 128-137, 2017.

10 Xu, X., Barsha, N.A.F. and Li, J.: Analyzing Regional Influence of Particulate Matter on the City of
11 Beijing, China, Aerosol Air Qual. Res., 8, 78-93, 2008.

12 Xu, J., Zhang, Q., Chen, M., Ge, X., Ren, J., and Qin, D.: Chemical composition, sources, and
13 processes of urban aerosols during summertime in northwest China: insights from high-resolution
14 aerosol mass spectrometry, Atmos. Chem. Phys., 14, 12593-12611, doi:10.5194/acp-14-12593-2014,
15 2014.

16 Xu, J., Shi, J., Zhang, Q., Ge, X., Canonaco, F., Prévôt, A. S. H., Vonwiller, M., Szidat, S., Ge, J.,
17 Ma, J., An, Y., Kang, S., and Qin, D.: Wintertime organic and inorganic aerosols in Lanzhou, China:
18 sources, processes, and comparison with the results during summer, Atmos. Chem. Phys., 16, 14937-
19 14957, doi:10.5194/acp-16-14937-2016, 2016.

20 Xu, W. Q., Sun, Y. L., Chen, C., Du, W., Han, T. T., Wang, Q. Q., Fu, P. Q., Wang, Z. F., Zhao, X. J.,
21 Zhou, L. B., Ji, D. S., Wang, P. C., and Worsnop, D. R.: Aerosol composition, oxidation properties,
22 and sources in Beijing: results from the 2014 Asia-Pacific Economic Cooperation summit study,
23 Atmos. Chem. Phys., 15, 13681-13698, doi:10.5194/acp-15-13681-2015, 2015.

24 Zhang, J. P., Zhu, T., Zhang, Q. H., Li, C. C., Shu, H. L., Ying, Y., Dai, Z. P., Wang, X., Liu, X. Y.,
25 Liang, A. M., Shen, H. X., and Yi, B. Q.: The impact of circulation patterns on regional transport

Atmospheric
Chemistry
and Physics
Discussions

1   pathways and air quality over Beijing and its surroundings, Atmos. Chem. Phys., 12, 5031–5053,

2   doi:10.5194/acp-12-5031-2012, 2012.

3   Zhang, R. Y., Wang, G. H., Guo, S., Zamora, M. L., Ying, Q., Lin, Y., Wang, W., Hu, M., and Wang,

4   Y.: Formation of urban fine particulate matter, Chem. Rev., 115, 3803–3855,

5   doi:10.1021/acs.chemrev.5b00067, 2015a.

6   Zhang, Y. J., Tang, L. L., Wang, Z., Yu, H. X., Sun, Y. L., Liu, D., Qin, W., Canonaco, F., Prévôt, A.

7   S. H., Zhang, H. L., and Zhou, H. C.: Insights into characteristics, sources, and evolution of

8   submicron aerosols during harvest seasons in the Yangtze River delta region, China, Atmos. Chem.

9   Phys., 15, 1331-1349, doi:10.5194/acp-15-1331-2015, 2015b.

10 Zhang, Y. J., Tang, L. L., Yu, H. X., Wang, Z., Sun, Y.L., Qin, W., Chen, W. T., Chen, C. H., Ding,

11 A. J., Wu, J., Ge, S., Chen, C., and Zhou, H. C.: Chemical composition, sources and evolution

12 processes of aerosol at an urban site in Yangtze River Delta, China during wintertime, Atmos.

13 Environ., 123, 339-349, 2015c.

14 Zhao, P., Dong, F., Yang, Y., He, D., Zhao, X., Zhang, W., Yao, Q., and Liu, H.: Characteristics of

15 carbonaceous aerosol in the region of Beijing, Tianjin, and Hebei, China, Atmos. Environ., 71, 389–

16 398, 2013a.

17 Zhao, P. S., Dong, F., He, D., Zhao, X. J., Zhang, X. L., Zhang, W. Z., Yao, Q., and Liu, H. Y.:

18 Characteristics of concentrations and chemical compositions for PM2.5 in the region of Beijing,

19 Tianjin, and Hebei, China, Atmos. Chem. Phys., 13, 4631–4644, doi:10.5194/acp-13-4631-2013,

20 2013b.

21 Zhou, W., Jiang, J., Duan, L., and Hao, J.: Evolution of submicron organic aerosols during a complete

22 residential coal combustion process, Environ. Sci. Technol., 50, 7861–7869, 2016.

23

24

25

Atmospheric
Chemistry
and Physics
Discussions

1   Table 1. The fine PM mass concentrations and fractional contribution of different composition in

2   different locations.

City	Season	NR-PM$_1$ ($\mu g\ m^{-3}$)	OA %	SO$_4^{2-}$ %	NO$_3^-$ %	NH$_4^+$ %	Cl$^-$ %	Ref.
Beijing	Winter, 2010	60	54	14	11	12	9	Hu et al., 2016a
Beijing	Winter, 2011	59	51	13	17	14	5	Sun et al., 2015
Beijing	Winter, 2012	66.8	52	14	16	13	5	Sun et al.,2013
Beijing	Winter, 2012	79	52	17	14	10	7	Wang et al., 2015
Beijing	Winter, 2013	77	50	19	16	12	3	Sun et al., 2014
Beijing	Winter, 2013	13.0	52	17	14	10	7	Jiang et al., 2015
Beijing	Winter, 2013	64	60	15	11	8	6	Sun et al., 2016
Beijing	Winter, 2014	75[a]	56	16	10	7	11	Elser et al., 2016
Beijing	Summer, 2011	80	32	28	21	17	2	Hu et al., 2016a
Beijing	Summer, 2012	52	41	14	25	17	3	Sun et al., 2015
Lanzhou	Winter, 2014	57.3	55	13	18	11	3	Xu et al., 2016
Lanzhou	Summer,	24	53	18	11	13	5	Xu et al., 2014

	2012							
Ziyang	Winter, 2012	60	40	24	15	17	4	Hu et al., 2016b
Handan	Winter, 2015	178	47	16	15	13	9	Li et al., 2017
Shenzhen	Autumn, 2009	38.3	46	29	12	11	2	He et al., 2011
Shanghai	Summer, 2010	27	31	36	17	14	2	Huang et al., 2012
Nanjing	Summer, 2013	36.8	42	14	24	19	1	Zhang et al., 2015b
Hong Kong	Winter, 2012	14.5	33	40	10	16	1	Li et al., 2015b
Hong Kong	Summer, 2011	8.7	26	56	3	15	0.1	Li et al., 2015b
Paris	Winter, 2010	16.7	35	16	33	15	1	Crippa et al., 2013
Fresno, Califonia	Winter, 2010	11.8	67	3	20	8	2	Ge et al., 2012
Shijiazhuang	Winter, 2014	178	50	21	12	11	6	This study

1   ^{a}NR-PM$_{2.5}$

1
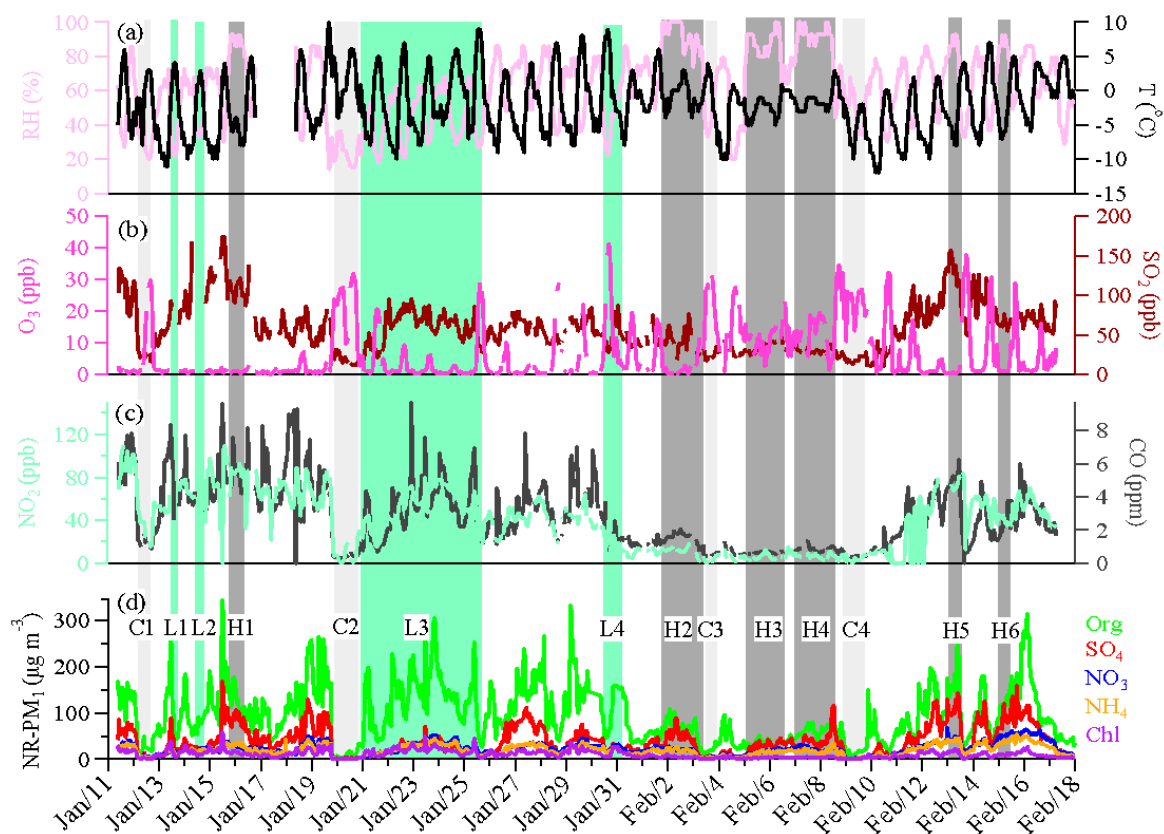
Fig. 1 Time series of relative humidity and temperature(a), O_3 and SO_2 (b), NO_2 and CO (c),

and the NR-PM$_1$ species (d) during the observation period. 6 high-RH (>80%) polluted episodes

(H1-H6), 4 low-RH (<60%) polluted episodes (L1-L4), and 4 clean episodes (C1-C4) are marked

for further discussion.
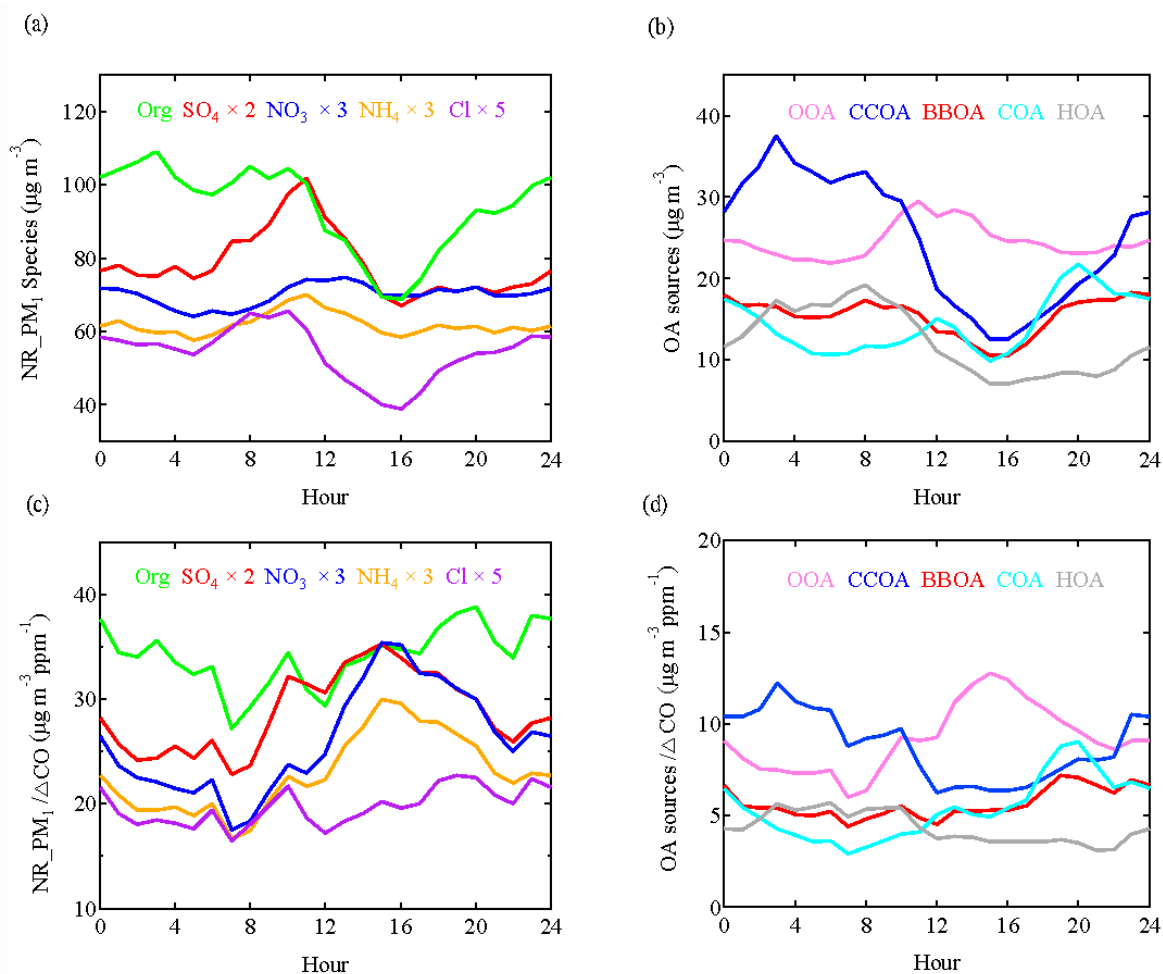
Fig. 2. Diurnal variations of NR-PM$_1$ composition (a), OA sources (b), NR-PM$_1$ species/ΔCO (C) and OA sources/ΔCO (d).
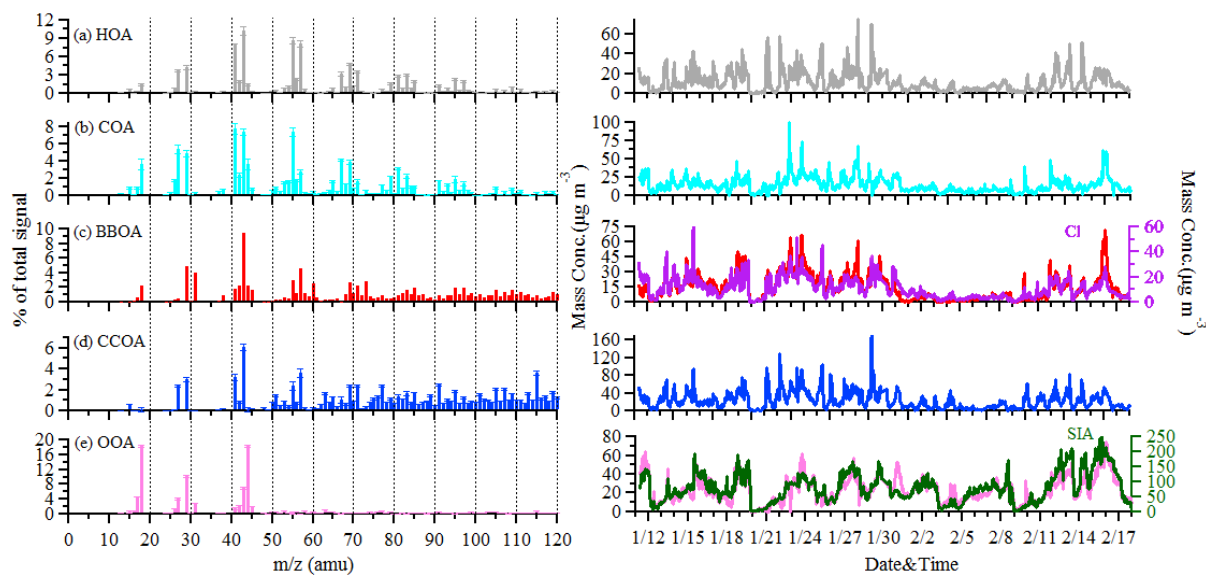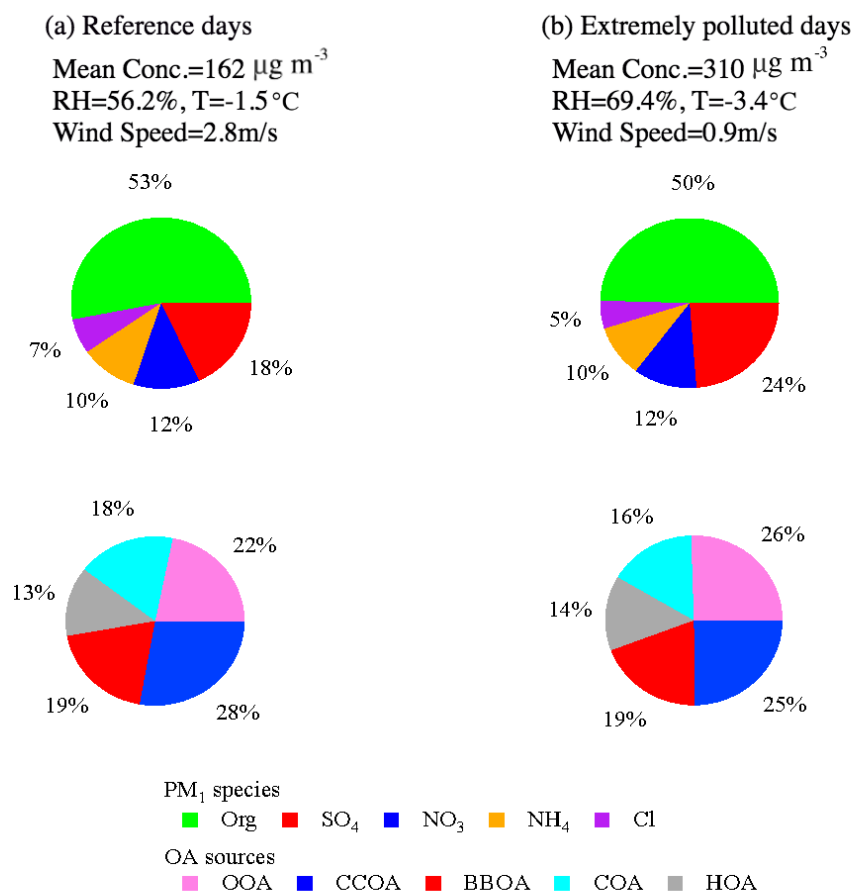
Fig. 3 Mass spectrums (left) and time series (right) of five OA sources. Error bars of mass spectrums represent the standard deviation of each *m/z* over all accepted solutions.

Atmospheric
Chemistry
and Physics
Discussions

Open Access

Fig. 4. Relative contributions of NR-PM$_1$ species and OA sources (OOA, CCOA, BBOA, COA and HOA) in reference days (a) and extremely polluted days (b). Extremely polluted days are defined as the daily average mass concentration of NR-PM$_1$ higher than the 75th percentile (237.3 μg m^{-3}) and the rest refers to the reference days. Data in the Spring Festival is excluded to eliminate the influence from a change of emission patterns in the holiday.

Atmospheric
Chemistry
and Physics
Discussions
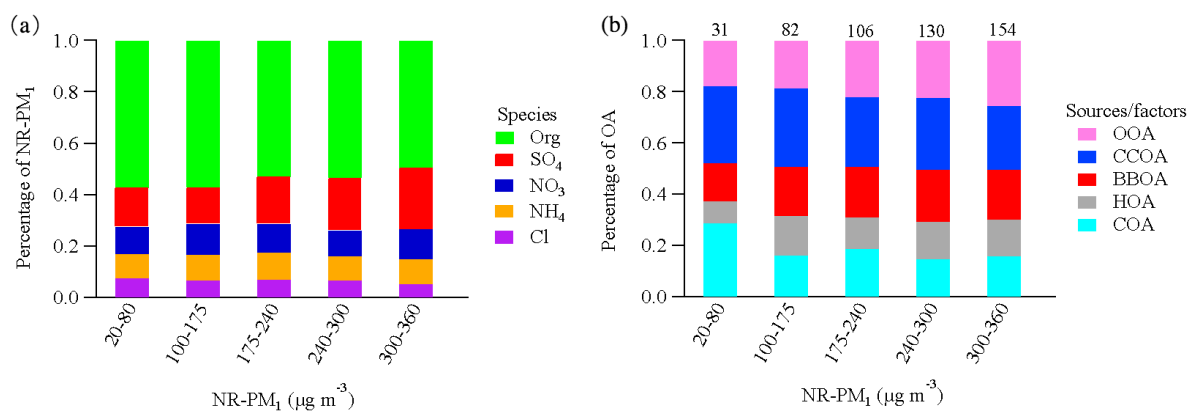
Fig. 5. Relative contributions of NR-PM$_1$ species (a) and OA sources (b) as a function of daily average NR-PM$_1$ mass concentrations. The numbers above the bars refer to the OA mass concentration (μg m^{-3}). Data in the Spring Festival is excluded to eliminate the influence from the change of emission patterns in the holiday.
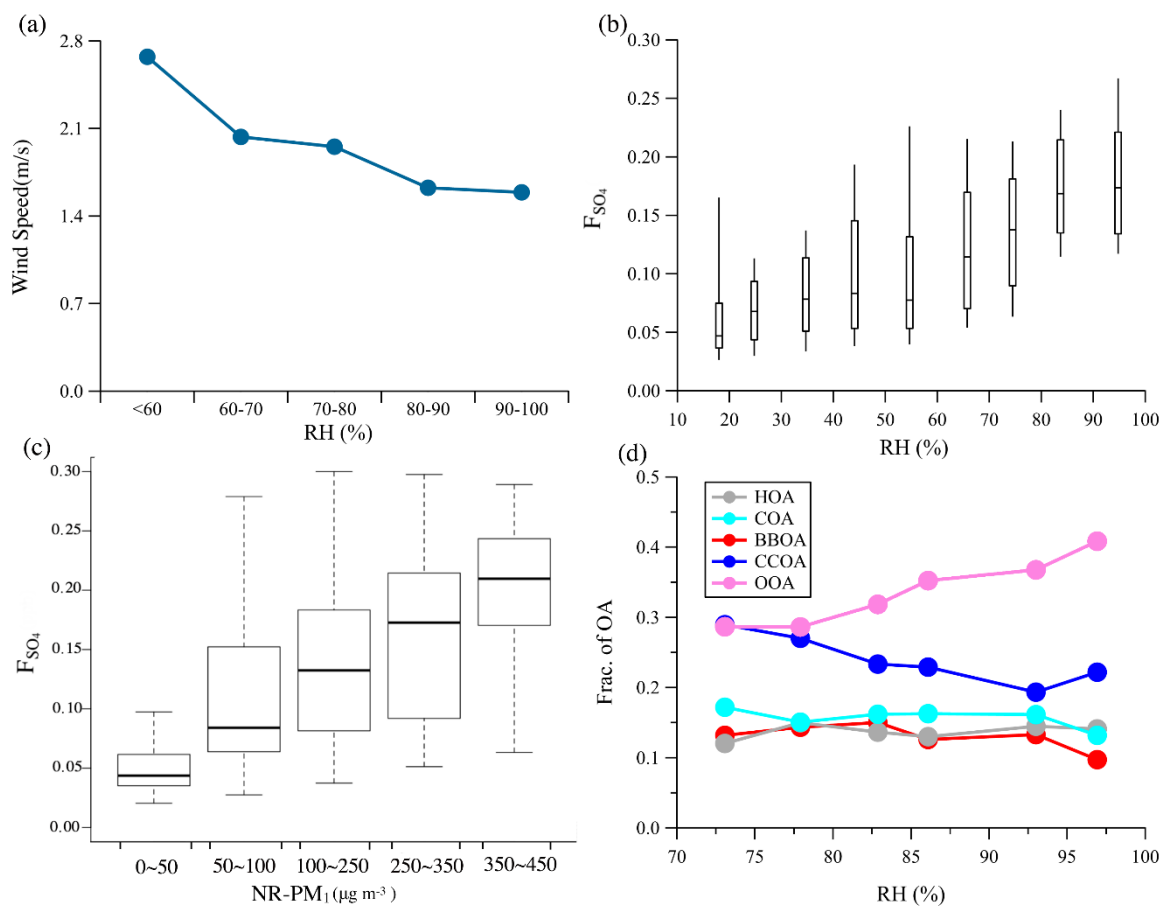
Fig. 6. Variations of wind speed as a function of RH (a), F_{SO4} as a function of RH (b) and of the NR-PM$_1$ mass concentrations (c), and the mass fraction of organic as a function of RH (d).

1
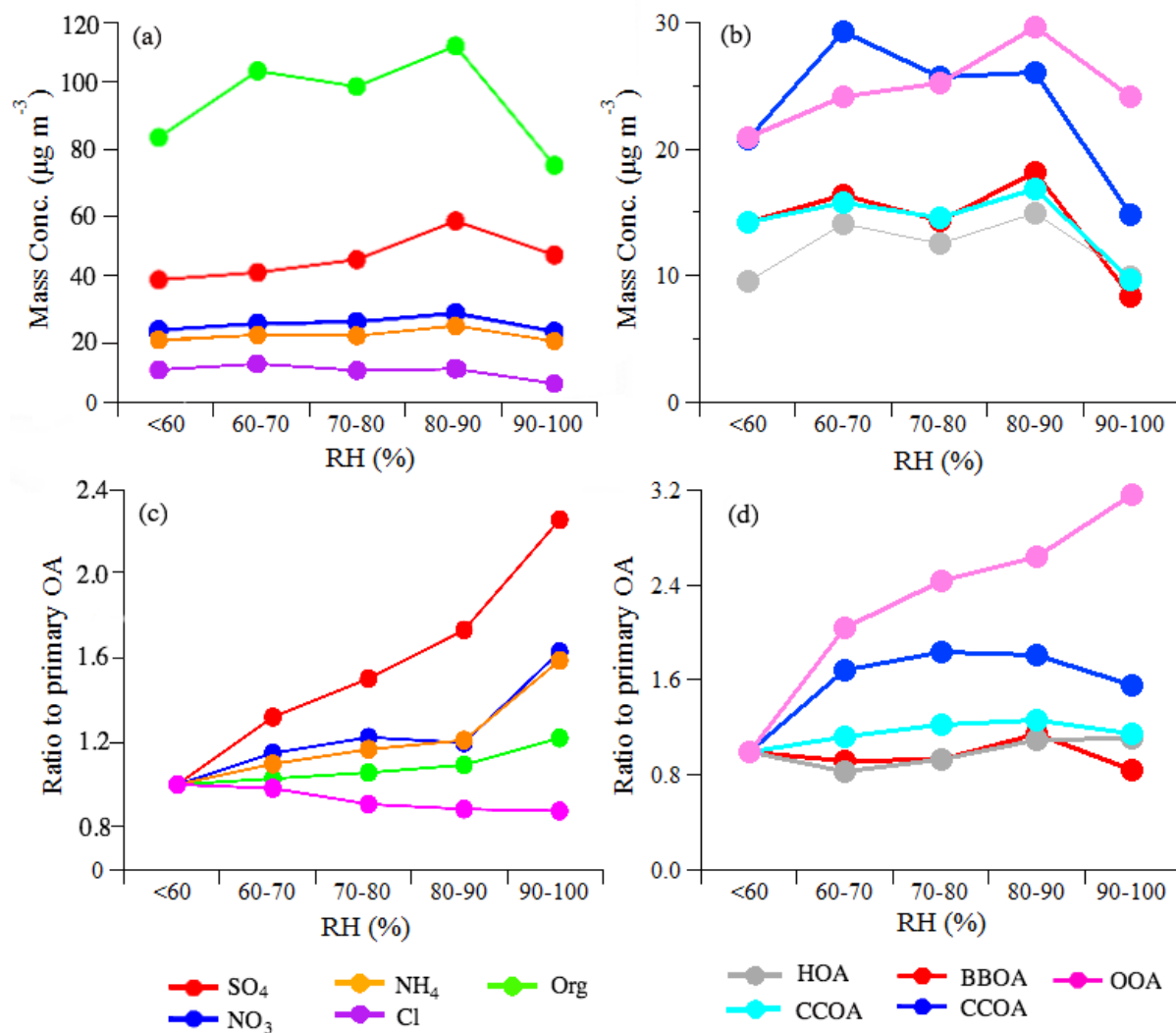
Fig. 7. The average mass concentration of NR-PM$_1$ species (a) and OA sources (b) as a function of RH. The average mass concentration of NR-PM$_1$ species (c) and OA sources (d) normalized to the sum of primary sources (HOA, COA, BBOA, and CCOA) as a function of RH. All ratios are further normalized to the values at the first RH bin (<60%) for the better illustration.

6

1
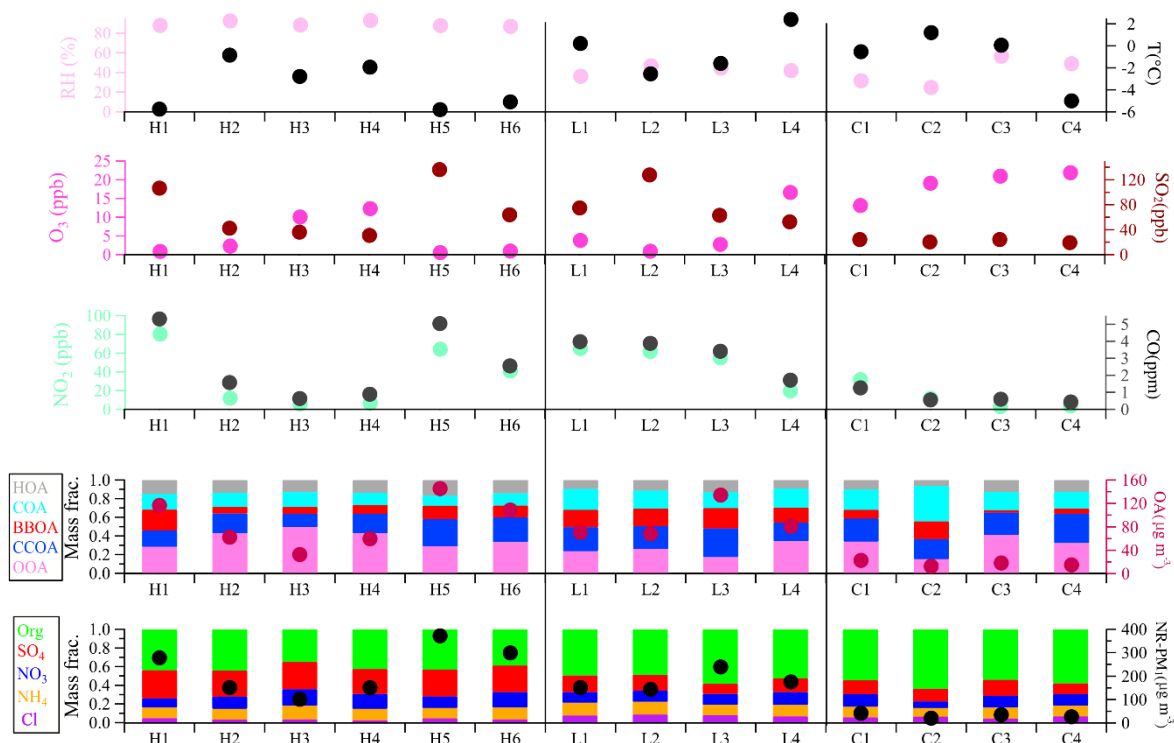
Fig. 8. Summary of relative humidity and temperature, gaseous species, organic sources and NR-PM$_1$ chemical composition for high-RH (H1-H6) polluted, low-RH (L1-L4), and clean (C1-C4) episodes.

Atmospheric
Chemistry
and Physics
Discussions

1
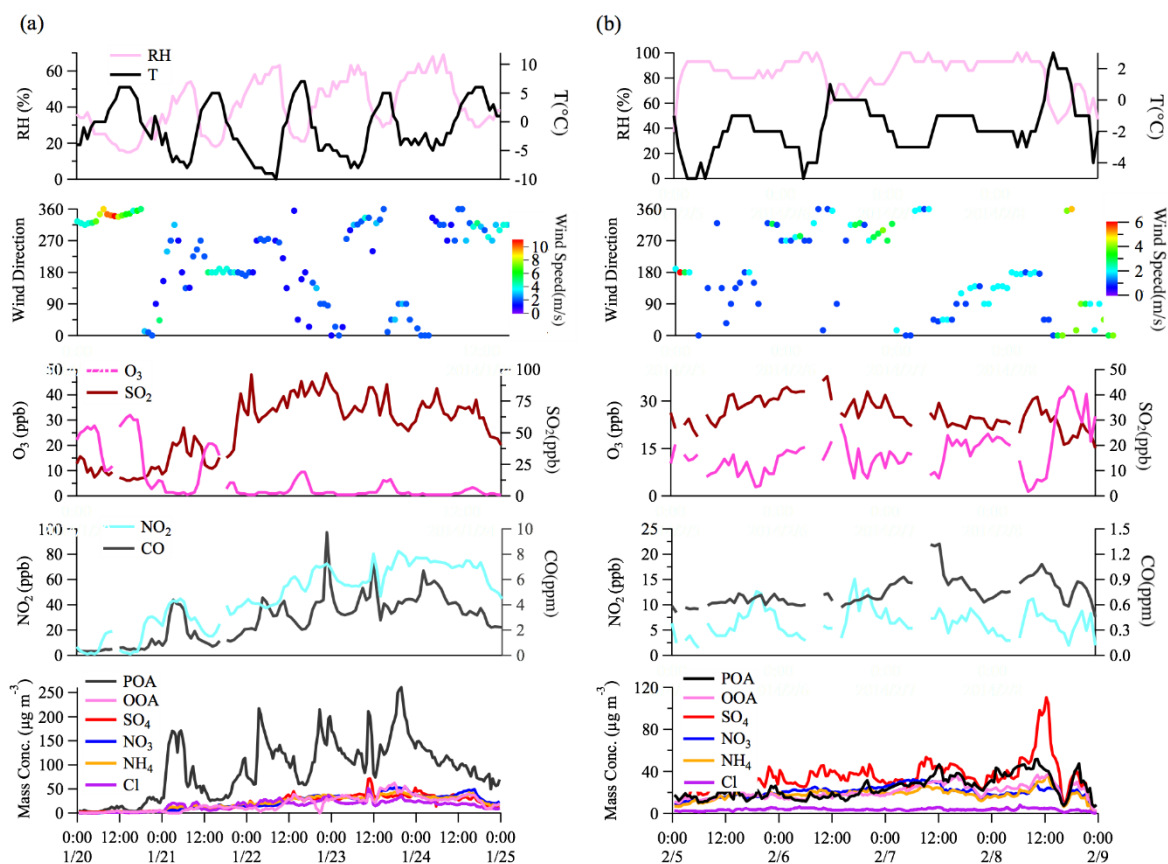
Fig. 9. Time series of meteorological factors (relative humidity, temperature, wind speed and wind direction), gaseous species, OA factors and NR-PM$_1$ chemical composition for the first period (average RH <50%) (a) and the second period (average RH>80%) (b).